Handa & Chawla, *Cogent Engineering* (2014), 1: 936996
http://dx.doi.org/10.1080/23311916.2014.936996

cogent engineering

PRODUCTION & MANUFACTURING | RESEARCH ARTICLE

Experimental evaluation of mechanical properties of friction welded AISI steels

Amit Handa[1*] and Vikas Chawla[2]

Abstract: In the present study, an experimental setup was designed and fabricated in order to accomplish friction welded joints between austenitic stainless steel and low-alloy steel. Thereafter, the effect of axial pressures on the mechanical properties of friction welded AISI 304 with AISI 1021 steels, produced by mechanical joining, have been investigated. Samples were welded under different axial pressures ranging from 75 to 135 MPa, at constant speed of 1250 rpm. The tensile strength, impact strength, and micro-hardness values of the weldments were determined and evaluated. Simultaneously, the fractrography of the tensile-tested specimens were carried out, so as to understand the failure analysis.

Keywords: friction welding, tensile strength, impact strength, micro-hardness, SEM, EDS

Received: 19 February 2014
Accepted: 12 June 2014
Published: 31 July 2014

*Corresponding author: Amit Handa, Mechanical Engineering, Punjab Technical University, Jalandhar Kapurthala Highway, Kapurthala, Punjab, India
E-mail: handaamit_2002@yahoo.com

Reviewing editor:
Zude Zhou, Wuhan University of Technology, China

Additional article information is available at the end of the article

1. Introduction

Joining of metals is one of the most essential needs of industry (Handa & Chawla, 2013). There are stringent needs of today's fabrication industry demand to use the cost-effective materials and procedures apart from quality and safety standards. Unfortunately, dissimilar metal welding has several fabrication and metallurgical drawbacks that can often lead to in-service failure. The most pronounced fabrication faults are hot cracks due to inadvertent use of incorrect welding electrodes, primarily carbon steel electrodes (Arivazhagan, Singh, Prakash, & Reddy, 2008). The use of carbon steel electrode results in the formation of very hard, crack-susceptible bulk structure on the stainless steel side of the dissimilar metal welding joint and along the fusion line of ferrite side of the joint discontinuous brittle and hard zones form (Arivazhagan et al., 2008). Such hard and brittle zones

ABOUT THE AUTHOR

Amit Handa born on 14 august 1976 at Patti, Punjab (India) worked on joining similar and dissimilar materials, especially by friction welding. He started working on this topic during his M.Tech thesis. Presently, he is a PhD research scholar at Punjab Technical University, Kapurthala, Punjab (India) and now working on the mechanical properties of dissimilar friction welded materials.

PUBLIC INTEREST STATEMENT

The joining of dissimilar metals is generally more challenging than that of similar metals because of difference in physical, mechanical, and metallurgical properties of the parent metals to be joined. The growing availability of new materials and higher requirement being placed on materials create a greater need for joints of dissimilar metals. Friction Welding is a class of solid-state welding process that generates heat through mechanical friction between two components with a relative velocity.

There are lots of industries which are using low-alloy steel to austenitic stainless steel. Advances in materials development and cooling schemes have led to increased operational temperatures of new generation gas turbine engines.

may render dissimilar metal welding susceptible to localized pitting corrosion attack, hydrogen embrittlement, sulfide stress cracking, and stress rupture, which often occurs in the weakened structure heat affected zone of the ferrite material of the dissimilar metal welding. Several in-service failures have been reported in the open literature (Arivazhagan et al., 2008). Thus, conventional fusion welding of many dissimilar metal combinations is not feasible owing to the formation of brittle and low-melting inter-metallic phases due to metallurgical incompatibility, wide difference in melting point, thermal mismatch, etc. (Meshram, Mohandas, & Reddy, 2007). Solid-state welding processes that limit the extent of intermixing are generally employed in such situations. Friction welding is one such solid-state welding process widely employed in such situations (Meshram et al., 2007).

Friction welding is one of the versatile and well-established welding processes (Meshram et al., 2007) that are capable of giving good quality welds; it gives solid state joining of the materials through the controlled rubbing of the interfaces. Due to this produced heat softens the material and brought the localized faces into the plasticized form which results in good quality welds (Sathiya, Aravindan, Haq, & Paneerselvam, 2009). In this process, heat energy is produced by the interconversion of mechanical energy into thermal energy at the interfaces of the rubbing components (Sahin, Akata, & Gulmez, 2007). In the present study low-alloy steel (AISI 1021) was welded with the austenitic stainless steel (AISI 304) at 1250 rpm under different axial pressures and afterwards the mechanical properties such as tensile strength, impact strength, and hardness were experimentally determined. The selected materials were used in the power generation industries for joining the nozzles to the safe ends.

2. Experimental setup

The experimental setup has been fabricated for the production of friction welded joints. For this, the conventional heavy duty direct drive lathe machine has been modified to suit the requirements of friction welding machine. The existing lathe machine model "Kirloskar [MK 1675]", speed range 30–1600 rpm, was used for this experimentation work. The modifications were done by fitting one more tail stock on the lathe machine. A load cell was designed and fitted between these two tail stocks, to measure the axial pressure applied on the specimens. For the fabrication of the load cell, the master brake cylinder made by TATA is used and the fluid filled inside the brake cylinder for transmitting the power is DOT-4. Pressure gauge, with a range of 0–150 MPa, is mounted on the brake cylinder so as to measure axial pressure. The two rods were used with this load cell for transmitting power, namely cylinder pushing rod and load transmitting rod. The handle of the original tail stock was removed to accommodate the load transmitting rod so that the barrel of this tail stock is being guided by the load transmitting rod. At the end of this barrel a specimen holder was fitted. This holder securely holds one of the specimens very rigidly. Figure 1 shows the fabricated friction welding setup.

Figure 1. Experimental setup of friction welding machine.

Table 1. Nominal (NCC) and actual chemical composition (ACC) of the materials

	Metal	Cr	Ni	C	Mn	Si	P	S	Fe
NCC	AISI 304	17–20	9–13	.08	2	.75	–	–	Balance
ACC	AISI 304	17.350	10.241	.04	1.880	.782	.021	.020	Balance
NCC	AISI 1021	–	–	.15–.25	.6–.9	–	–	–	Balance
ACC	AISI 1021	.002	.001	.221	.675	.231	.037	.035	Balance

Table 2. Experimental mechanical properties of the parent materials

Metal	Tensile strength (MPa)	Impact toughness (Charpy, J)	Impact toughness (Izod, J)	Micro-hardness (Hv)
AISI 1021	472.70	126	96	188
AISI 304	528.92	138	104	202

3. Development of welded joint

The bars were cleaned mechanically and chemically in order to make them free from oil, dirt, grease, etc. Samples of 20 mm in diameter and 100 mm in length were used, they were cut from the bar stocks and the facing operation was done on the lathe machine for the production of friction welds. These specimens were then fitted on the friction welding setup. Table 1 represents the NCC and the ACC of the materials. Furthermore, the experimental mechanical properties of the parent materials after the actual testing of parent materials considered for the investigation are reported in Table 2.

4. Results and discussion

Friction welded parts were subjected to variety of mechanical tests to determine their suitability for the anticipated service applications. They were necessary to carry out so as to ensure the quality, reliability, and strength of the welded joints. In our investigation, mechanical properties like tensile strength, impact strength, and micro-hardness were evaluated combined with the visual examination.

4.1. Visual examination

The friction welded specimens of five different welding combinations were prepared by varying the axial pressures at constant speed of 1250 rpm; it was found that a flash has been produced during friction welding process and the amount of flash increases with the rise in axial pressure. The formation of flash has been presented in Figure 2.

It has been observed from the experiments that the formation of flash is higher towards the low-alloy steel than the austenitic stainless steel in all cases. This might be attributed to the presence of Cr in austenitic stainless steel; as AISI 304 has lower thermal conductivity compared to low-alloy steel, for this reason, the formation of flash is higher on the AISI 1021 side than the AISI 304 side, also austenitic stainless steel has greater hardness at higher temperatures compared to low-alloy steels. For this reason, austenitic stainless steel does not undergo extensive deformation while the low-alloy steel undergoes extensive deformation. This phenomenon may be attributed to the low strength of AISI 1021 steel (Satyanarayana, Madhusudhan Reddy, & Mohandas, 2005).

4.2. Tensile testing

Tensile test carried for this study was performed on the Universal Testing Machine of the make HIECO, which had a capacity of 60 tons. The machine used for tensile testing had a computer interface and data was generated on the computer and on the basis of this data the graphs were plotted. The standard specimens using ASTM standards (www.astm.org/Standards/A370.htm) were followed

Figure 2. Friction welded specimens at various axial pressures showing formation of flash.

for preparing the samples. The gage lengths of the specimens were maintained according to the ASTM A370-12 standards by maintaining the weld interface at the center of the gage length. The sample was then fitted firmly between the jaws of the machine and load was applied. This test was carried out on the friction welded samples of AISI 304 with AISI 1021 materials to measure their strength in tension. In the test, specimens were subjected to axial tensile load till the failure occurred. It has been observed from the experimentation that with the increase in stress, the strain also goes on increasing; also, when the stress increases to its maximum value it starts declining but the strain continuously increases until the fracture occurs; similar trends have been reported in the literature (Özdemir, 2005). Figure 3 shows the variation of stress vs. strain behavior at different axial pressures, it depicts that with the increase in stress the strain increases. During tensile testing, brittle fracture appeared at 75 and 90 MPa axial pressures and the joint failed on the weld interface without showing any necking; whereas, at an axial pressure of 105 MPa, the joint also failed from the weld interface but little necking appeared at the interfaces; whereas, cup and cone fractures observed at pressures of 120 and 135 MPa. The tensile strength of these two specimens was found to be very

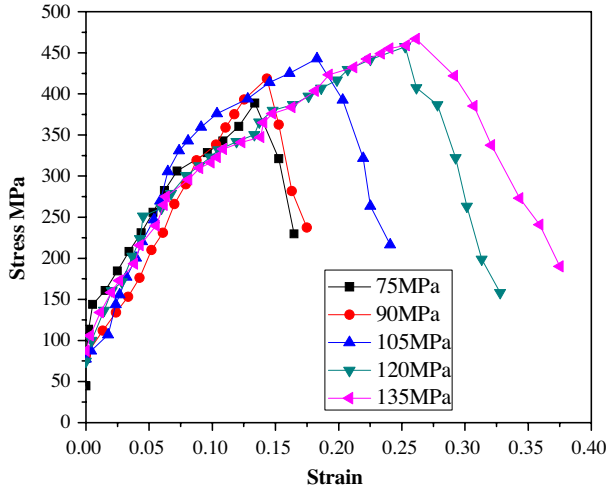

Figure 3. Stress strain behavior at different axial pressures.

Table 3. Tensile strength values of the friction welded joints

Sample No.	Axial pressure (MPa)	Peak load (kN)	Peak displacement (mm)	Peak strain	Peak stress (MPa)	Time (s)	Fracture location
S1-S2	75	47.72	8.24	.1648	388.85	16	Weld interface
S1-S2	90	51.37	8.74	.1748	418.59	18	Weld interface
S1-S2	105	54.36	12.04	.2408	442.96	23	Weld interface
S1-S2	120	56.14	16.39	.3278	457.46	31	Weaker parent metal
S1-S2	135	57.29	18.76	.3752	466.83	34	Weaker parent metal

close to the tensile strength of the weaker parent material. This might be attributed to the increase in the axial pressures; more mass in terms of elemental diffusion from austenitic stainless steel to low-alloy steel is thought to be transferred out of the interface due to more friction, thus, increasing the tensile strength. Tensile strength obtained from the specimens varied from 388.85 to 466.83 MPa, as has been shown in Table 3; similar results have been reported in the literature (Arivazhagan, Singh, Prakash, & Reddy, 2011). The value of strain varied from .1628 to maximum of .3752 depending upon the axial pressure used. It also depicts that the specimen welded at 135 MPa shows the maximum ductile behavior and maximum strength was also achieved at the same parameters. Table 3 shows the tensile strength values of the friction welded specimens. It has also been observed that the maximum time taken before the tensile fracture occurs was 34 s and that was also obtained at 135 MPa axial pressure.

Figure 4 shows the variation between the load and the time taken before its fracture, it depicts that the maximum load carried by the specimen was 57.29 kN and the maximum time taken by the specimen was 34 s before failure. Both of these values were also found at 135 MPa axial pressures. It also depicts that with the increase in axial pressure, the time taken before failure continuous to increase, and as the axial pressure increases beyond 105 MPa, there is abrupt rise in time taken, although there was not much variation in time at 120 and 135 MPa but still the time goes on increasing. Also, these are the two axial pressures at which the specimens were broken not from the weld interface but from the weaker metal.

To confirm the visual inspection of failure, the fracture analysis was done. For that scanning electron microscope (SEM) of JEOL model No. JSM-6610LV coupled with EDS was used. The SEM and EDS analyses were carried out to show the fracture behavior of tensile test which justifies the visual

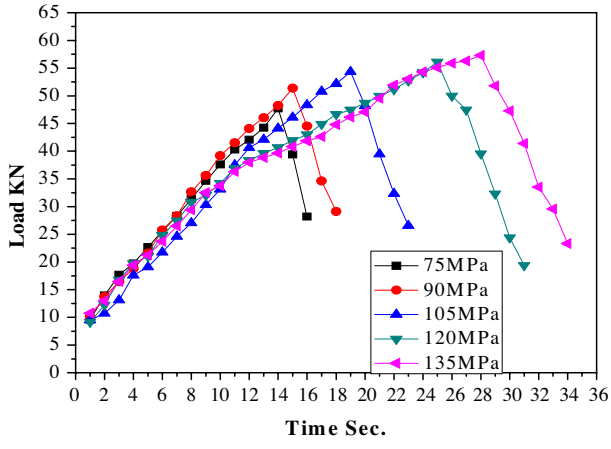

Figure 4. Variation of load vs. time at different axial pressures.

inspection results of brittle and ductile failures. The magnified images were captured at the fractured locations taken at 1,500x magnification. The effect of tensile strength has been observed on the fractured surface appearance. In Figure 5(A), the fractograph indicates the pure brittle failure, no voids are visible on the surface and dimples are also absent. The EDS performed at two locations indicates the enrichment of Cr indicating the fracture may take place at the joint. This may be due to the formation of martensite at the interface of the joints (Özdemir & Orhan, 2005), also has been observed from the tensile test that minimum time has been taken by the specimen before getting failed. Figure 5(B) also indicating the brittle failure behavior even though very small amount of dimples appears to be present, indicating the sign of river like pattern, which depicts the brittleness of

Figure 5. SEM images with EDS (A–E) at 1,500x magnification during tensile testing at different axial pressures.

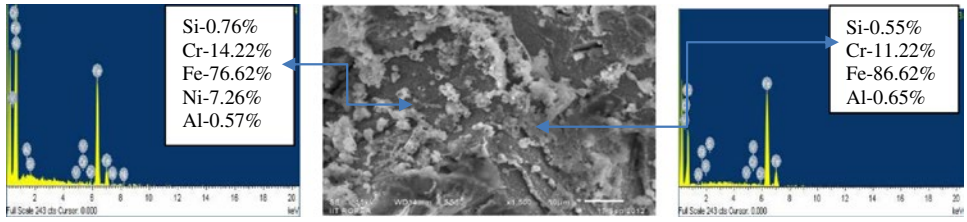

(A) SEM image at 75MPa axial pressure

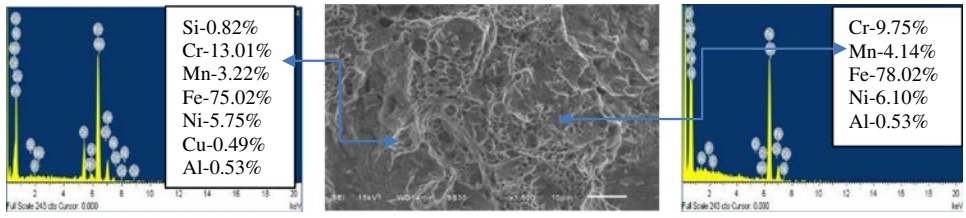

(B) SEM image at 90MPa axial pressure

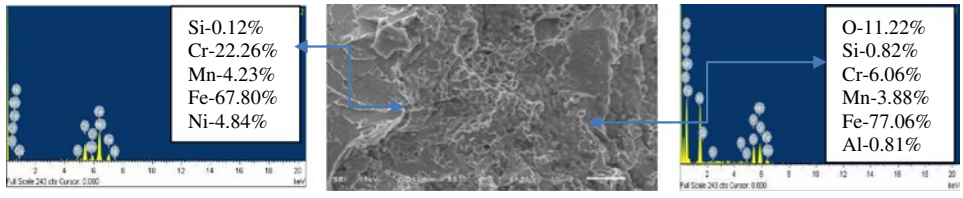

(C) SEM image at 105MPa axial pressure

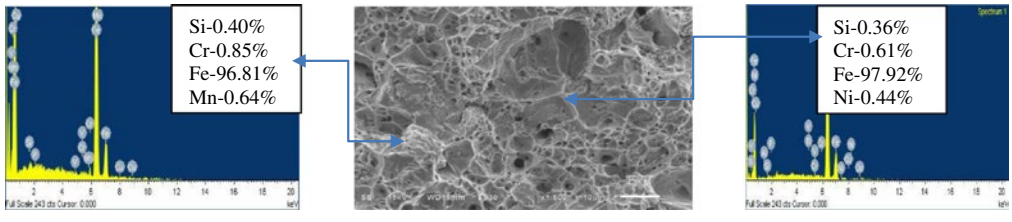

(D) SEM image at 120MPa axial pressure

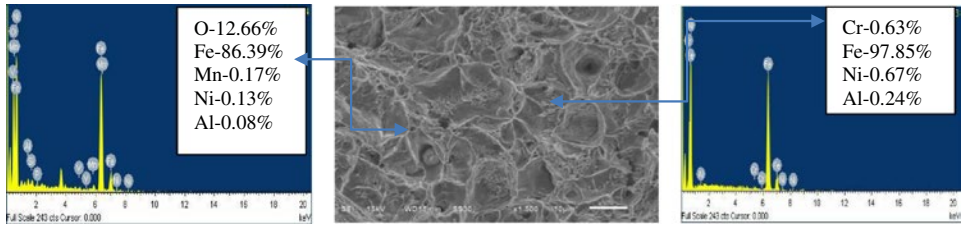

(E) SEM image at 135MPa axial pressure

the joint. Figure 5(C) reveals cleavage pattern as well as dimples at various locations. The river lines or stress lines are steps between cleavage or parallel planes, which are always converged in the direction of local crack propagation leading to the brittle failure of the specimen; this indicates that the fracture may have occurred by the mixed phenomenon i.e. quasi-cleavage fracture mechanism (Chawla, Batra, Puri, & Chawla, 2008). Figure 5(D) and (E) represents dimpled pattern showing ductile fracture. Figure 5(D) and (E) also depicts that the dimples are deep as compared to Figure 5(C) indicating more ductility. In Figure 5(D) and (E), the failure was located in AISI 1021 side and therefore ductile fracture similar to that of pure Fe was observed (Meshram et al., 2007). The EDS analysis performed on these locations indicate up to 96% of Fe, depicting the failure may take place towards 1021 side.

4.3. Micro-hardness testing

For micro-hardness testing, Vickers hardness testing machine was used. In this test, a square-based pyramid type diamond indenter was used and the hardness variation on the weld interface as well as along the axis of shaft at the intervals of 1 mm on both the parent materials was obtained by applying a constant load of 500 gf. The indentations were made at the weld interface and along both the parent materials in longitudinal direction at fixed intervals, so as to find out the effect of heat on the hardness values. The results obtained are reported in Table 4 and on the basis of the obtained values of hardness, the graph was plotted. Figure 6 shows the hardness variations on both the sides of the friction welded joint. Figure 6 depicts that AISI 1021 shows less hardness as compared to the AISI 304. This decrease in hardness may be attributed to recrystallization process taking place at the heat affected zone towards the low-alloy steel

Table 4. Hardness values of the friction welded joints

Specimen	Axial pressure (MPa)	Micro-hardness at a distance (mm) from weld interface towards AISI 304 material				Micro-hardness at the weld interface	Micro-hardness at a distance (mm) from weld interface towards AISI 1021 material			
		4	3	2	1	Weld interface	1	2	3	4
S1-S2	75	200	200	217	229	233	214	207	193	174
S1-S2	90	202	208	216	233	239	214	210	191	177
S1-S2	105	202	214	226	240	235	220	219	193	173
S1-S2	120	200	210	226	239	242	222	217	187	171
S1-S2	135	204	219	231	241	248	234	226	195	179

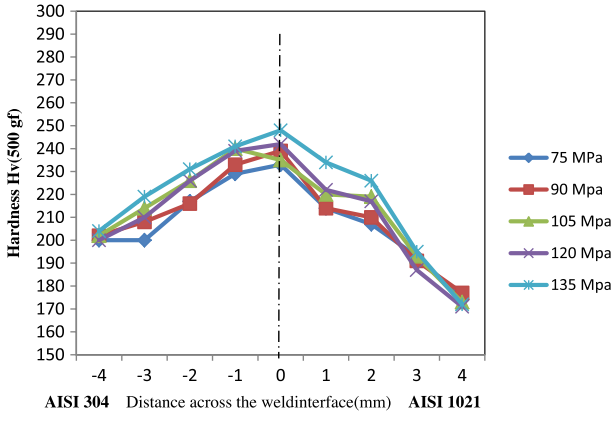

Figure 6. Variation of hardness values at different axial pressures.

(Ananthapadmanaban, Seshagiri Rao, Abraham, & Prasad Rao, 2009). It has also been observed that the maximum hardness was obtained at the weld interface for all the joints (Özdemir & Orhan, 2005). The peak hardness of friction welded joins increases with the increase in burn-off length (Arivazhagan et al., 2011), our plot follows the similar trends. Burn-off length is the axial shortening of the length during friction welding and it was observed that with the increase in burn-off length, a soft region appears on the austenitic stainless steel adjacent to the weld interface. The formation of soft region can be attributed to decarburization (Arivazhagan et al., 2008). This may be occurred by the presence of heat as the thermal conductivity of the material is relatively low (Satyanarayana et al., 2005). In addition to that the higher values of hardness at the weld interface were probably due to the oxidation process which takes place during friction welding (Ates, Turker, & Kurt, 2007).

4.4. Impact toughness

This test was carried out on the pendulum type single blow impact testing machine so as to measure their notch impact toughness. Again, the samples were prepared according to the ASTM standards (www.astm.org/Standards/A370.htm) maintaining the notch at the center of the weld interface. The specimens were supported at both ends as a simple supported beam and were broken by a falling pendulum on the face opposite to the notch and the energy absorbed by the specimen was noted down. Along with this Izod test was also performed in this test the specimens were vertically placed and the notch was facing towards the falling pendulum. The notch impact toughness tests were carried out to find amount of energy absorbed during fracture. For this, Charpy and Izod impact tests were carried out so as to find out the amount of energy absorbed by the specimens before failure. The samples were prepared for impact testing according to the ASTM standards A370-12. The results of both Charpy and Izod impact results in terms of fracture energies have been reported in Table 5. As it can be seen from Table 5 that the Charpy toughness of the welded parts is slightly higher than the Izod impact toughness, this may be the reason for the placement of the impact samples towards the impact load. In case of Charpy impact test, the specimen is simply supported and the blow of the hammer was done on the opposite side of the specimen, while in case of Izod Impact test, the specimen is placed as a cantilever and the notch of the specimen is facing towards the blow of impact. Figure 7 reveals that the Charpy impact strength firstly increases with the increase in axial pressure, and then remains constant up to 105 MPa pressure and after that with the increase in axial pressure declines a bit. When the pressure increases beyond 120 MPa, there was sharp decline in the impact strength. Quite similar trends have been recorded during Izod impact testing, Figure 7 shows that the decrease in impact strength is marginal at 90 MPa and then it remains constant up to 120 MPa and then similar like Charpy sudden decline in toughness was noticed with the further increase in the axial pressure. The similar results have been reported in the literature (Satyanarayana et al., 2005). It has also been observed that with the increase in the axial pressure, the flash increases, and experimentally, it has been found that with the increase in the flash, the impact strength decreases (Arivazhagan et al., 2008, 2011).

Table 5. Hardness values of the friction welded joints

S. No.	Specimen	Axial pressure (MPa)	Energy absorbed (Charpy, J)	Energy absorbed (Izod, J)
1	S1-S2	75	23	17
2	S1-S2	90	24	16
3	S1-S2	105	24	16
4	S1-S2	120	23	16
5	S1-S2	135	19	13

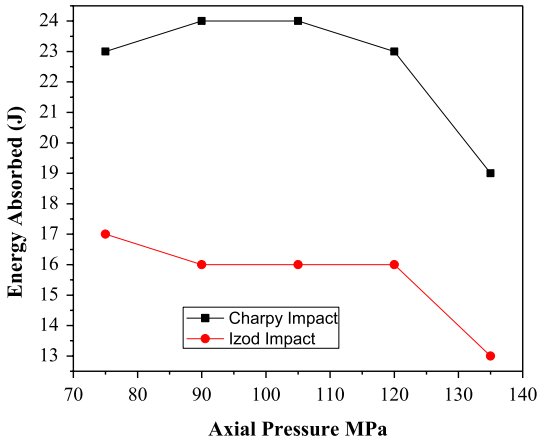

Figure 7. Variation of impact toughness values at different axial pressures.

5. Conclusions

The following conclusions are made from the study:

(1) Continuous drive friction welding machine was found to be successful for the production of austenitic–ferritic stainless steel weldments.

(2) The axial pressure has been found to be an influential parameter for the friction welding process, which has been optimized for the process based on the results of the present study. The mechanical properties of the friction welds were found to vary with the applied axial pressure, which indicates that axial pressure is an important welding parameter.

(3) With the increase in axial pressure, the tensile strength increases, the time taken before fracture also increases with the same and maximum time was achieved at 135 MPa, which was 34 s. The maximum available tensile strength which was 466.83 MPa, was also available at this axial pressure.

(4) It has been observed that the impact toughness for the weldments follows the reverse trend, it declines as axial pressure increases. The maximum impact toughness values of 23 and 17 J both for Charpy and Izod impact were available at 75 MPa.

(5) With the increase in the axial pressure, the hardness at the center of weld cross-section increases. The maximum value of hardness, which was found to be 248 Hv, was available at 135 MPa axial pressure.

Funding
The authors received no direct funding for this research.

Author details
Amit Handa[1]
E-mail: handaamit_2002@yahoo.com
Vikas Chawla[2]
E-mail: vikkydmt@gmail.com
[1] Mechanical Engineering, Punjab Technical University, Jalandhar Kapurthala Highway, Kapurthala, Punjab, India.
[2] DAV College of Engineering & Technology, Kanina, Haryana, India.

Citation information
Cite this article as: Experimental evaluation of mechanical properties of friction welded AISI steels, A. Handa & V. Chawla, *Cogent Engineering* (2014), 1: 936996.

References

Ananthapadmanaban, D., Seshagiri Rao, V., Abraham, N., & Prasad Rao, K. (2009). A study of mechanical properties of friction welded mild steel to stainless steel joints. *Materials & Design, 30*, 2642–2646. http://dx.doi.org/10.1016/j.matdes.2008.10.030

Arivazhagan, N., Singh, S., Prakash, S., & Reddy, G. M. (2008). An assessment of hardness, impact strength, and hot corrosion behaviour of friction-welded dissimilar weldments between AISI 4140 and AISI 304. *The International Journal of Advanced Manufacturing Technology, 39*, 679–689. http://dx.doi.org/10.1007/s00170-007-1266-7

Arivazhagan, N., Singh, S., Prakash, S., & Reddy, G. M. (2011). Investigation on AISI 304 austenitic stainless steel to AISI 4140 low alloy steel dissimilar joints by gas tungsten arc, electron beam and friction welding. *Materials & Design, 32*, 3036–3050. http://dx.doi.org/10.1016/j.matdes.2011.01.037

Ates, H., Turker, M., & Kurt, A. (2007). Effect of friction pressure on the properties of friction welded MA956 iron-based superalloy. *Materials & Design, 28*, 948–953. http://dx.doi.org/10.1016/j.matdes.2005.09.015

Chawla, V., Batra, U., Puri, D., & Chawla, A. (2008). To study the effect of austempering temperature on fracture behavior of Ni–Mo austempered ductile iron. *Journal of Minerals & Materials Characterization & Engineering, 7*, 307–316.

Handa, A., & Chawla, V. (2013). Mechanical characterization of friction welded dissimilar steels at 1000 rpm. *Materials Engineering* [Materiálové inžinierstvo], *20*, 102–111.

Meshram, S. D., Mohandas, T., & Reddy, G. M. (2007). Friction welding of dissimilar pure metals. *Journal of Materials Processing Technology, 184*, 330–337. http://dx.doi.org/10.1016/j.jmatprotec.2006.11.123

Özdemir, N. (2005). Investigation of the mechanical properties of friction-welded joints between AISI 304L and AISI 4340 steel as a function rotational speed. *Materials Letters, 59*, 2504–2509. http://dx.doi.org/10.1016/j.matlet.2005.03.034

Özdemir, N., & Orhan, N. (2005). Microstructure and mechanical properties of friction welded joints of a fine-grained hypereutectoid steel with 4% Al. *Journal of Materials Processing Technology, 166*, 63–70. http://dx.doi.org/10.1016/j.jmatprotec.2004.07.095

Sahin, M., Akata, H. E., & Gulmez, T. (2007). Characterization of mechanical properties in AISI 1040 parts welded by friction welding. *Materials Characterization, 58*, 1033–1038. http://dx.doi.org/10.1016/j.matchar.2006.09.008

Sathiya, P., Aravindan, S., Haq, A. N., & Paneerselvam, K. (2009). Optimization of friction welding parameters using evolutionary computational techniques. *Journal of Materials Processing Technology, 209*, 2576–2584. http://dx.doi.org/10.1016/j.jmatprotec.2008.06.030

Satyanarayana, V. V., Madhusudhan Reddy, G., & Mohandas, T. (2005). Dissimilar metal friction welding of austenitic–ferritic stainless steels. *Journal of Materials Processing Technology, 160*, 128–137. http://dx.doi.org/10.1016/j.jmatprotec.2004.05.017

Cogent Engineering **(ISSN: 2331-1916) is published by Cogent OA, part of Taylor & Francis Group.**